# Fabrication of Surface Relief Optical Elements in Ternary Chalcogenide Thin Films by Direct Laser Writing

I. Voynarovych[1], R. Poehlmann[2], S. Schroeter[2] and M. Vlcek[1]
[1]*Department of General and Inorganic Chemistry, Faculty of Chemical Technology, University of Pardubice, Studentska 573, Pardubice, Czech Republic*
[2]*Leibniz Institute of Photonic Technology, Albert-Einstein-Str. 9, Jena, Germany*

Keywords: Direct Laser Writing, Chalcogenide Glasses, Patterned Structures.

Abstract: Direct laser writing with a continuous-wave high intensity and over-band gap laser is applied to realize surface relief optical elements in ternary *As-S-Se* and *Ge-As-S* thin chalcogenide films. The topology of created structures in dependence on the experimental conditions is investigated. Analyses indicate that the formation mechanisms of the surface patterns are thermally induced processes generated by the local heating and involve thermoplastic deformation, mass flow induced by the surface tension gradient and evaporation. Diffractive gratings with a period of 2.56 μm, depths of up to 100 nm, and different periodic surface structures were patterned at the surface of 1 μm thick films. The spectral dependencies of diffraction efficiency were measured and discussed.

## 1 INTRODUCTION

The chalcogenide glass (ChG) family exhibits several interesting properties that can be exploited e.g. in optical communication, optical sensing, high density optical recording, and optical lithography. In particular, their excellent infrared transparency up to 12–20 μm, large third order susceptibility, high refractive index (usually 2–3.2), and ability to undergo significant irradiation induced structural modifications make chalcogenide glass films good candidates for the fabrication of all-optical switches (Harbold, 2002) and integrated optical elements (Meneghini, 1998; Viens, 1999). Optical integrated as well as diffractive elements in chalcogenide glasses have been fabricated by several techniques including interference photolithography (Utsugi, 1975; Chomat, 1976; Palyok, 1999), ion implantation and direct ion/laser beam writing (Schroeter, 2007; Nordman, 1996). The direct laser writing (DLW) by a tightly focused laser beam has been intensively developed during the last decades as an efficient way to produce 2D and 3D microstructures. It attracts high interest due to its inherent advantages like high precision, moderate cost, high speed, and high flexibility (Thiel, 2010; Van, 2009).

Among all the variety of chalcogenide glasses (ChGs), i.e. glasses containing chalcogen elements (e.g. *S, Se, Te*), arsenic trisulfide $As_2S_3$ ($As_{40}S_{60}$) is one of the most studied and well-known. A particular interest attract ternary compositions based on $As_2S_3$ for which the substitution of *S* by *Se* gives the possibility to monotonically change optical properties such as the band gap energy, from 2.4 eV down to 1.8 eV, and the refraction coefficient from 2.3 up to 2.7 (Gonzalez-Leal, 2003), whereas the substitution of tri-coordinated *As* by four-coordinated *Ge* causes the glass network to change from a two-dimensional layered structure to a three-dimensional structure with a more rigid network resulting in a significant change of the thermodynamic properties such as softening temperatures, viscosity etc. (Feltz, 1993; Tatsumisago, 1990).

In this paper we compare the behavior of different ternary *As-S-Se* as well as *Ge-As-S* thin films under cw laser exposure in dependence on the writing conditions and demonstrate the possibility to fabricate surface relief diffractive optical elements by DLW.

## 2 EXPERIMENTAL

Bulk samples of *As* and *Ge* based glasses from


Voynarovych I., Poehlmann R., Schroeter S. and Vlcek M..
Fabrication of Surface Relief Optical Elements in Ternary Chalcogenide Thin Films by Direct Laser Writing.
DOI: 10.5220/0005404001340139
In *Proceedings of the 3rd International Conference on Photonics, Optics and Laser Technology* (PHOTOPTICS-2015), pages 134-139
ISBN: 978-989-758-093-2

ternary systems *As-S-Se* and *Ge–As–S* were prepared by conventional melt-quenching method from high purity (5 N) elements in evacuated quartz ampoules for 8 h at 650°C (As based samples) or 1000°C (Ge based samples) in a rocking furnace. Thin-film samples were prepared by vacuum evaporation of the bulk glassy materials onto clean glass substrates. The thermal evaporation process was performed within a coating system (Tesla Corporation, model UP-858) at a pressure of about $10^{-3}$ Pa. During the deposition process the substrates were conveniently rotated by means of a planetary rotation system to ensure high homogeneity of the film thickness. The deposition rate was in the range 1–2 nm/s, measured continuously using the quartz microbalance technique. The thickness of the thin films was about 1 μm

The laser lithography system DWL 66, Heidelberg Instruments Mikrotechnik GmbH, equipped with a vertically polarized continuous-wave He-Cd laser (λ=442 nm) was used for the exposures. The maximal laser power available after the writing objective to expose the samples was $P_{max}$=1.8 mW. The laser beam was focused to a spot diameter of about 640 nm by an objective with a focal length of 4 mm and a numerical aperture of 0.85. The focus distance of the objective is controlled by an air gauge based autofocus system. The applied exposure laser power P was tuned by a rotable polarizer in steps of 10% from $P_{max}$ down to $0.4 \cdot P_{max}$, resulting in spot intensities between $5.6\times10^5$ W/cm$^2$ and $2.2\times10^5$ W/cm$^2$. Structures were patterned at writing speeds of 25-75 mm/s. An atomic force microscope (Ultraobjective SIS attached to an optical microscope) was used to investigate the morphology of the corrugated surface of the thin films. The transmission spectra and diffraction efficiencies were measured with the fiber coupled spectrometer EPP2000 (StellarNet Inc.)

## 3 RESULTS AND DISCUSSION

To compare the behavior of thin chalcogenide films with different optical and thermodynamic properties under the irradiation with an over band-gap cw laser a series of single lines was written with different laser intensities ranging from $2.2\times10^5$ to $5.6\times10^5$W/cm$^2$ on each of the samples of the different investigated compositions. Created surface structures were investigated by atomic force microscopy, and the geometrical profiles of each line were taken by scanning in the direction perpendicular to the laser beam movement. The analysis of such profiles shows that they can be divided into three main groups (see inset of Fig.1) indicating various possible formation mechanisms depending on the laser intensity as well as on the properties of the distinct thin film.

The curve 1 in the inset of Fig.1 represents a typical profile for photo-induced expansion that appears at all used intensities for *Ge-As-S* thin films and at low intensity of the writing laser beam for *As-S-Se* compositions. In this case the shape of the corrugated structure follows the Gaussian intensity profile of the laser beam. The dependences of the height of the emergent elevations ('hills') on the laser intensity are shown in the upper part of Fig. 1 for different compositions.

The curve 2 in the inset of Fig.1 represents emerging profiles for the case that a groove with a simultaneously appearing rim surrounding the center of the laser spot is created. Formation of such a profile is typical only for *As-S-Se* thin films above an experimentally determined threshold value of $2.8\times10^5$ W/cm$^2$, whereas for Ge-based ternary compositions only the creation of grooves without any rim (see curve 3) was observed. The magnitude of the groove depth obtained from the AFM images, is represented in the lower part of Fig. 1 as a function of exposure intensity for the different compositions.

As we used an over-bandgap writing laser the beam energy was totally absorbed within a small volume of the thin film. The penetration depth $d_{pd}$ of the He-Cd laser beam was evaluated according to the Beer-Lambert law as $d_{pd}=1/\alpha$ ($\alpha$ – absorption coefficient). For $As_{40}S_{60-x}Se_x$ compositions $d_{pd}$ varies from 240 nm (x=0) down to 80 nm (x=60) and for the *Ge*-based compositions $d_{pd}$ is 240 nm almost independent on the composition. Because of the extremely high intensity and the total absorption of the light within a very small volume, the thin chalcogenide film can be locally and rapidly heated up to temperatures above $T_g$, or even to temperatures where material decomposition and evaporation take place. The temperatures on the surface at the center of a stationary Gaussian heat source for a semi-infinite solid can be calculated as (Carslaw, 1959):

$$T(t) = \frac{P_a}{Kw\pi^{3/2}} atan\left(\frac{2\sqrt{D*t}}{w}\right), \qquad (1)$$

where, $t$ – duration of laser interaction with the thin film, $w$ – waist of the laser beam (0.64 μm), $K$ and $D$ are the thermal conductivity and diffusivity of the glass substrate ($1\times10^{-2}$ W/K*cm and $5.33\times10^{-3}$ cm$^2$/s respectively), $P_a=P(1-R)$, where $P$ is the power of the incident beam and $R$ the reflectivity at the air-film interface. The potential of this model to

describe the thermal evolution in chalcogenide thin films during over-band gap cw laser irradiation was demonstrated (Nordman, 1999). The temperatures calculated for our experimental conditions are shown as the top axis on Fig.1.

The most common and simple, but remarkably accurate, relation between the changing rate of any kinetic parameter and the temperature change is given by the Arrhenius equation: $F=A\cdot exp(-E_a/k_BT)$, where $F$ is a rate constant, $A$ the pre-exponential factor, $E_a$ the activation energy for the change to take place, $T$ the temperature, and $k_B$ the Boltzmann constant.

As can be seen from Eq. (1), the temperature on the thin film surface is proportional to the laser beam intensity. The straight line dependences for the depth of grooves for *As*-based thin films as well as of the height of hills for *Ge*-based compositions (see Fig.1) on the inverse of the beam intensity (and thus on the inverse temperature) clearly show that both parameters obey Arrhenius' equation and we can thus conclude that the formation mechanisms of the patterned structures are thermally-induced processes.

The temperature of the thin film's surface for exposure power levels at which solely expansion was observed is close to the glass softening temperature (180-210 ºC range for *As-S-Se* and 230-440 ºC for *Ge-As-S* ternary compositions (Feltz, 1993). The most realistic mechanism is in this case the thermoplastic deformation proposed in Refs. (Zhao, 2013; Shiu, 1999). According to this mechanism, a locally heated volume expands preferably in the direction to the film's interface with air because of the suppresion of expansion in other directions by the unheated glass and the plastic deformation due to the yield stress of heated and thus softened material.

When, however, the surface temperature of the chalcogenide film at still higher laser intensities exceeds the softening temperature of a given glass composition the viscosity of the exposed material begins to decrease (Feltz, 1993) and thus melts in the irradiated spot area resulting in a different surface corrugation mechanism. The processes of surface corrugation for the case of a locally molten material area were theoretically and experimentally investigated by several authors (Blom, 1983; Cline, 1981; Anthony, 1977). According to the proposed model, the molten material is pulled from the center of the molten spot by a shear stress and forms the rim surrounding the central hole (curve 2 in the inset of Fig.1), which is the result of a surface tension and a viscosity gradient, in turn resulting from a temperature gradient induced by the focused laser beam with a Gaussian intensity profile. In the case of *Ge*-based ternary compositions, the more rigid glass structure and thus the smaller temperature dependence of the viscosity (Tatsumisago, 1990) in combination with a counterflow induced by capillary pressure can prevent the viscous flow in the given temperature region.

At the highest intensities available for exposures only for *As*-based compositions the process of decomposition/evaporation−back-condensation takes place when the temperature exceeds the experimentally determined threshold temperature of about 370 ºC.

Having in detail investigated the power dependence of the resulting structural parameters we have chosen the maximal available intensity of $5.6x10^5$ W/cm$^2$ and a scan speed of 75 mm/s to pattern surface relief gratings with a period of $\Lambda$=2.54 μm and an area of 5x5 mm$^2$ into ternary *As-S-Se* and *Ge-As-S* thin films. In Fig.2 are shown the AFM images of diffraction gratings with a period $\Lambda$=2.54 μm patterned by DLW with the chosen writing parameters on the surface of $As_2S_3$ (a) and $Ge_{25}As_{15}S_{60}$ (b) thin films. The groove depth for the Ge-containing thin films was only up to 12 nm and the gratings exhibit thus only very low diffraction efficiency. But these gratings can be further developed by wet or dry etching. However, the depth of grooves for a diffraction grating on *As-S-Se* thin films can vary from a few nanometers up to about 100 nm by choosing appropriate writing parameters.

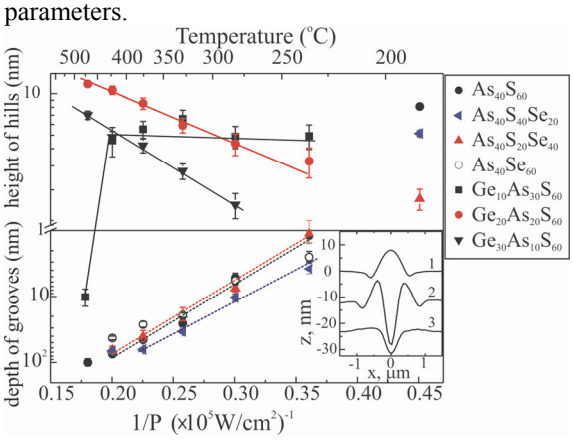


Figure 1: Dependences of depth of grooves and height of hills of corrugated structures on the exposed intensity (bottom axis) and calculated surface temperature (top axis) for different ternary Ge-based and As-based thin films.

For the used writing parameters given above the quality of the grating surface for the $As_2S_3$ film is very good, whereas for lower writing speeds evaporation and back-condensation processes start to

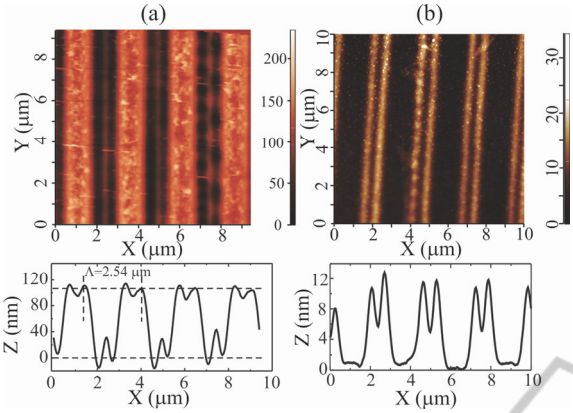


Figure 2: AFM scan and averaged profile of the surface relief grating formed by DLW on the surface of $As_2S_3$ (a) and $Ge_{25}As_{15}S_{60}$ (b) thin films written with an intensity of $5.6\times10^5$ W/cm$^2$ and a scan speed 75 mm/sec.

take place and randomly spread small material particles emerge at the surface. This causes an increased level of stray light deteriorating the diffraction properties.

Binary surface relief diffractive elements can exhibit very high diffraction efficiency. Let us consider the case of a surface relief phase grating on a thin film evaporated on a usual glass substrate as shown in Fig. 3.

To define whether a grating is thin or thick the parameter $Q$ can be used (Collier, 1971):

$$Q = \frac{2\pi\lambda D}{n\Lambda^2\cos(\theta_0)} \tag{2}$$

where $\lambda$ is the free space wavelength, $D$ the grating thickness, $n$ the average refractive index. For our structural parameters $Q$ is less than 1 defining the grating as thin. Applying the scalar diffraction theory and neglecting the reflection at the air-film interface for a thin binary surface relief grating with a fill factor $f$, the zero-order transmittance efficiency $\eta_0$ into the grating material can be derived as (Jing, 2011)

$$\eta_0 = 1 - 2f(1-f)\cdot(1-cos\Delta\varphi), \tag{3}$$

whereas for the other diffraction orders $m$ the efficiency $\eta_{m\neq0}$ is given by:

$$\eta_{m\neq0} = \frac{(1-\cos 2m\pi f)(1-cos\Delta\varphi)}{m^2\pi^2}, \tag{4}$$

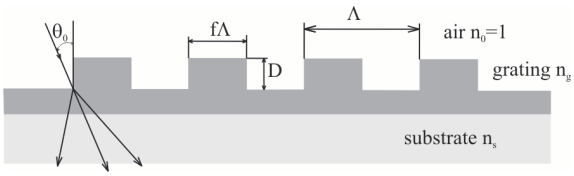


Figure 3: Binary diffraction grating.

with

$$\Delta\varphi = \frac{2\pi D(n_f - 1)}{\lambda} \tag{5}$$

As can be seen from Eq. 4, the maximal diffraction efficiency into the first order is

$$\eta_{\pm1} = 4/\pi^2 \approx 0.405$$

for the case $f$=0.5 and $\Delta\varphi$=π.

Approximating the grating profile shown in Fig. 2(a) by a binary structure with $D$=90 nm, and using the index of refraction for $As_2S_3$ (Laniel, 2003) $\Delta\varphi$ decreases from 0.96·π at $\lambda$=400 nm to 0.295·π at $\lambda$=1000 nm.

Taking also into account the Fresnel reflection R at the interface of the chalcogenide film with the air for the case of normal incidence ($\theta_0$=0) the efficiencies calculated from Eqs. (3) and (4) are reduced by the factor $1$-$R$, with

$$R = \left(\frac{n_f - 1}{n_f + 1}\right)^2 \tag{6}$$

The diffraction efficiencies into the chalcogenide film according to the scalar diffraction theory as calculated using Eq. (3) to Eq. (6) are represented in Fig. 4.

For comparison are also shown the results of a rigorous calculation applying the Rigorous Coupled Wave Analysis (RCWA) (Moharam, 1982).

The main reason for the differences between the simulations and the measured diffraction efficiencies is that the calculations are made for the diffraction into the chalcogenide film and do not take into account that the diffracted powers in the experiment are measured after propagation through the unstructured part of the layer and the glass substrate into air. For the short wavelength range the absorption of $As_2S_3$ (Laniel, 2003) reduces the transmitted power significantly. With increasing wavelength the absorption of $As_2S_3$ is rapidly decreasing, however the reflections at the interfaces chalcogenide glass / glass substrate and substrate/air can lower the transmission. Accordingly the experimental results are spectrally modulated in similarity with the transmission of the unstructured thin film also shown in Fig. 4.

In the focus of interest are currently also photonic crystals composed of periodic microstructures that affect the propagation of electromagnetic and/or plasmonic waves in a specific manner and offer unique properties for the realization of different photonic devices. Examples of such periodic surface microstructures that were

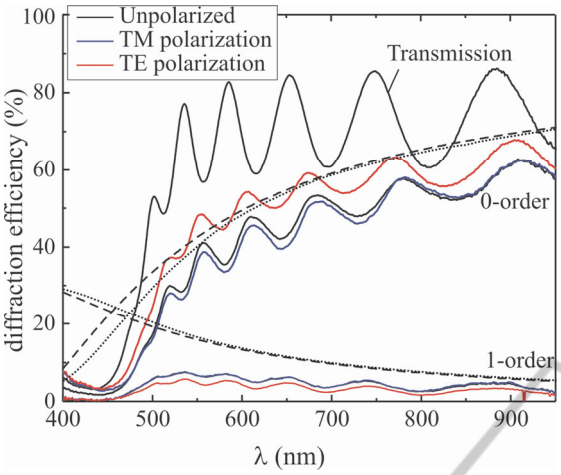


Figure 4: Spectral dependence of thin film transmission, 0-order and 1-order diffraction efficiencies (solid lines) measured for normal incidence at a grating prepared by DLW on the surface of an $As_2S_3$ thin film with an intensity of $5.6\times10^5$ W/cm$^2$ and a scan speed of 75 mm/sec and diffraction efficiencies calculated with scalar and rigorous diffraction theories (dashed and dotted line respectively).

fabricated by DLW with a resolution down to about 1 μm in a $Ge_{20}As_{20}S_{60}$ chalcogenide thin film are shown in Fig. 5. However, for practical applications a post-exposure etching process would be required in order to significantly increase the depth of the structures.

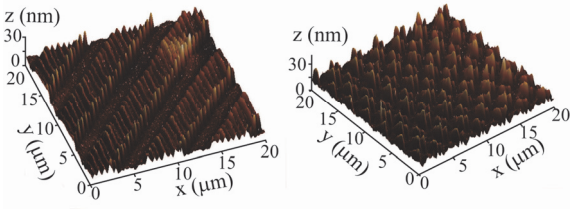


Figure 5: AFM images of periodic arrays with different pattern shapes created by DLW in a $Ge_{20}As_{20}S_{60}$ thin film.

## 4 CONCLUSIONS

The surface corrugation processes induced by the irradiation of ternary $As_{40}S_{60-x}Se_x$ and $Ge_xAs_{40-x}S_{60}$ thin films with a continuous wave tightly focused overband-gap laser emitting at 442 nm were investigated.

Analyses of the topology of the created structures indicate that the formation mechanisms of the surface patterns are thermally induced processes generated by the local heating and involve thermoplastic deformation, mass flow induced by surface tension gradient and decomposition/ evaporation mechanism.

By tuning the laser power diffractive optical elements like diffraction gratings with a period of 2.56 μm and various depths or periodic surface microstructures with feature sizes down to less than 1 micrometer and different shapes were patterned.

The zero- and first-order diffraction efficiencies were measured for a diffractive grating in a $As_2S_3$ thin film within the visible and near infrared spectral range. A maximal value of 8% for the first diffraction order was measured.

## ACKNOWLEDGEMENTS

This work was supported by the grant CZ.1.07/2.3.00/30.0058 from the Czech Ministry of Education, Youth and Sports

## REFERENCES

Anthony T. R. and Cline H. E., 1977 'Surface rippling induced by surface tension gradients during laser surface melting and alloying', *J. Appl. Phys.*, vol. 48, pp.3888-3894.

Blom G. M., 1983 'Hole formation in tellurium alloy films during optical recording', *J. Appl. Phys.*, vol.54, pp.6175-6182.

Carslaw H. S. and Jaeger J. C., 1959. *Conduction of Heat in Solids*, Oxford University, Oxford, 2nd ed.

Chomat H., Lezal D., Gregora I., and Srb I., 1976 'Relief holograms in thin films of amorphous $As_2Se_3$ under high laser exposures', *J. Non-Cryst. Solids*, vol.20, pp.427-437.

Cline E., 1981 'Surface rippling induced in thin films by a scanning laser', *J. Appl. Phys.*, vol.52, pp.443-448.

Collier R. J., Burckhardt C. B., Lin L. H. 1971. *Optical holography*, Academic Press, - Technology & Engineering, 605 p.

Feltz A. 1993 'Amorphous Inorganic Materials and Glasses', VCH Weinheim/VCH Publishers, New York,. 446 p.

Gonzalez-Leal J.M., Prieto-Alcon R., Angel J.A., Marquez E., 2003 'Optical properties of thermally evaporated amorphous $As_{40}S_{60-x}Se_x$ films', *Journal of Non-Crystalline Solids*, vol. 315 pp.134–143.

Harbold J. M., Ilday F. O., Wise F. W., Sanghera J. S., Nguyen V. Q., Shaw L. B., Aggarwal I. D., 2002 'Highly nonlinear *As-S-Se* glasses for all-optical switching', *Opt. Lett.*,vol. 27, pp.119-121.

Jing X., Jin Y., 2011 'Transmittance analysis of diffraction phase grating', *Applied Optics*, vol.50. pp. c11-c18.

Laniel J. M., Menard J., Turcotte K., Villeneuve A., Vallee R., Lopez C., Richardson K. A., 2003 'Refractive index measurements of planar chalcogenide thin film', *J. Non-Cryst. Solids*, vol. 328,

pp. 183–191.

Meneghini C., Villeneuve A., 1998 '$As_2S_3$ photosensitivity by two-photon absorption: holographic gratings and self-written channel waveguides', *J. Opt. Soc. Am. B* vol. 15, pp. 2946-2950.

Moharam M. G., and Gaylord T. K., 1982 'Diffraction analysis of dielectric surface-relief gratings', *J. Opt. Soc. Am.* vol.72, pp.1385-1392.

Nordman N., Salminen O., Kuittinen M., and Turunen J.,1996 'Diffractive phase elements by electron-beam exposure of thin $As_2S_3$ Films', *J. Appl. Phys.*, vol. 80, pp.1079-1080.

Nordman O. and Nordman N., 1999 'Hole formation induced by 488.0-nm light in 10-mm-thick amorphous as-evaporated $As_2S_3$ films', *Phys. Rev. B: Condens. Matter.*, vol. 60, pp.2833-2838.

Palyok V., Mishak A., Szabo I., Beke D. L., Kikineshi A., 1999 'Photoinduced transformations and holographic recording in nanolayered *a-Se*/$As_2S_3$ and *AsSe*/$As_2S_3$ films', *Appl. Phys. A*, vol. 68, pp. 489-492.

Schroeter S., Vlcek M., Poehlmann R., Fiserova A., 2007 'Efficient diffractive optical elements in chalcogenide glass layers fabricated by direct DUV laser writing', *J. Phys. Chem. Solids*, vol. 68, pp.916–919.

Shiu T., Grigoropoulos C. P., Cahill D. G., and Greif R., 1999 'Mechanism of bump formation on glass substrates during laser texturing', *J. Appl. Phys.*, vol. 86, pp.1311-1316.

Tatsumisago M., Halfpap B. L., Green J. L., Lindsay S. M., and Angell C. A., 1990 'Fragility of *Ge-As-Se* glass-forming liquids in relation to rigidity percolation, and the Kauzmann paradox', *Phys. Rev. letters*, vol. 64, pp.1549-1552.

Thiel M., Fischer J., von Freymann G., Wegener M., 2010, 'Direct laser writing of three-dimensional submicron structures using a continous-wave laser at 532nm', *Appl. Phys. Lett.* vol. 97, p.221102.

Utsugi Y. & Zembutsu S., 1975 'Relief type diffraction grating by amorphous chalcogenide films', *Appl. Phys. Lett.* vol. 27, pp.508-510.

Van Gough D., Juhl A. T. and Braun P. V. 2009, 'Programming structure into 3D nanomaterials', *Materials today*, vol. 12, p.28.

Viens J-F., Meneghini C., Villeneuve A., Galstian T. V., Knystaunas E. J., Duguay M. A., Richardson K. A., Cardinal T., 1999 'Fabrication and characterization of integrated optical waveguides in sulfide chalcogenide glasses', *J. Lightwave Technology* vol. 17, pp.1184-1191.

Zhao D., Jain H., Malacarne L. C., and Pedreira P. R. B., 2013 'Role of photothermal effect in photoexpansion of chalcogenide glasses', *Phys. Status Solidi B*, vol. 250, pp.983–987.